photons, however, into a higher triplet state, irreversible photochemistry does occur and the reactions shown in Scheme II can proceed.

With use of the holographic technique, the wavelength dependence of this photochemistry can be investigated. The results are summarized in Figure 13. We clearly see that excitation of the absorption band at 320 nm results in observable photochemistry, while excitation of the band with a maximum at 520 nm does not. The short-wavelength triplet–triplet absorption band has been assigned to an $n\pi^*$ state, as has the lowest triplet state, and the long wavelength band is attributed to a $\pi\pi^*$ state.[16]

### Concluding Remarks

The holographic technique has proven to be a simple but sensitive technique for investigating photochemical reactions in the solid state. Since it is a zero-background technique, it can be used to follow photochemical changes that are too small to detect by other means. Reactions that do not result in holograms are not detected by the technique and their presence does not interfere with the results.

The technique can be extended in a variety of ways. By chopping the coherent light source and measuring the transient holograms, one might hope to follow photochemistry in liquids. The hologram growth can be followed as a function of temperature in order to measure activation energies for photochemical reactions. This would be particularly useful in the case of higher triplet states. There are of course a variety of other circumstances in which the holographic technique may prove useful.

*I am deeply indebted to all of my co-workers whose names appear in the references cited in this paper for their contributions to the development of the holographic technique. I am also grateful to G. C. Bjorklund and H. E. Hunziker for their critical reading of the manuscript. In addition I would like to acknowledge the partial financial support of the Office of Naval Research and the U.S. Army Research Office.*

# Chemical Applications of Picosecond Spectroscopy

E. F. HILINSKI and P. M. RENTZEPIS*

*Bell Laboratories, Murray Hill, New Jersey 07974*

*Received July 12, 1982*

Ever since the possibility of measuring the duration of light pulses emerging from mode-locked lasers existed, picosecond spectroscopy[1] has been developing as a field of science through which one may view fleeting elementary events. A powerful technique that permits direct observation of processes occurring in the range of $10^{-12}$ s has become an experimental reality. For understanding the physical and chemical changes that occur within a specific system, it is no longer necessary to probe the mechanism indirectly by frequently inconclusive kinetic arguments based upon chemical reactions. The primary events of most processes such as dissociation, photosynthesis, and polymerization, whose macroscopic significance are well realized, may be identified and understood by means of picosecond spectroscopy. Direct observation of intermediate species involved in chemical and biological processes and measurement of their formation and decay kinetics can be made while the reaction proceeds by means of absorption, emission, and Raman picosecond spectroscopy.

The areas of chemistry, physics, and biology that have benefitted from picosecond studies are very large and continuously growing. The vast numbers of applications include studies of excited-state relaxation, cage effects, proton-transfer reactions, solvation of electrons, photosynthesis, vision, and nonlinear effects. This Account shall not even attempt to review this field of science but shall be restricted to some techniques and a few exemplary studies of chemical events that were performed primarily in our laboratories.

### Experimental Methods

Picosecond laser systems in use today vary widely. Most commonly they are based on either solid-state oscillators, such as $Nd^{3+}$:silicate glass or $Nd^{3+}$:YAG, or synchronously pumped dye lasers. Each system possesses its own desirable features in terms of repetition rate, energy output, pulse width, and reliability. $Nd^{3+}$:YAG lasers, while producing pulses with a full width at half-maximum (FWHM) of ~20–40 ps, generate pulses with energy equal to that of a $Nd^{3+}$:glass oscillator but of narrower bandwidth (0.3 $cm^{-1}$) and permit repetition rates on the order of 10 Hz. Mode-locked dye lasers are capable of ~1-ps pulses of low energy, which, in principle, can be tuned in wavelength over the range of the visible and ultraviolet spectrum,

Edwin Hilinski received his B.S. in Chemistry from Wilkes College. With Jerome Berson as his research advisor, he obtained his Ph.D. in 1982 from Yale University. Currently, he is a postdoctoral member of the technical staff at Bell Laboratories.

Peter M. Rentzepis is head of the Physical and Inorganic Chemistry Research Department at Bell Telephone Laboratories, Murray Hill, NJ. He is currently involved in picosecond spectroscopy research using lasers. Dr. Rentzepis holds over 25 patents and has published more than 200 articles. In addition to being affiliated with several universities as a visiting professor or advisor, he is editor of several technical journals and a fellow of the New York Academy of Science, the National Academy of Science, and the American Physical Society. He has been the recipient of three honorary doctorate degrees and has been accorded many awards, including the Scientist of the Year award in 1977 and the Peter Debye Award in Physical Chemistry in 1982.

(1) Rentzepis, P. M. *Chem. Phys. Lett.* **1968**, 2, 37.

0001-4842/83/0116-0224$01.50/0 

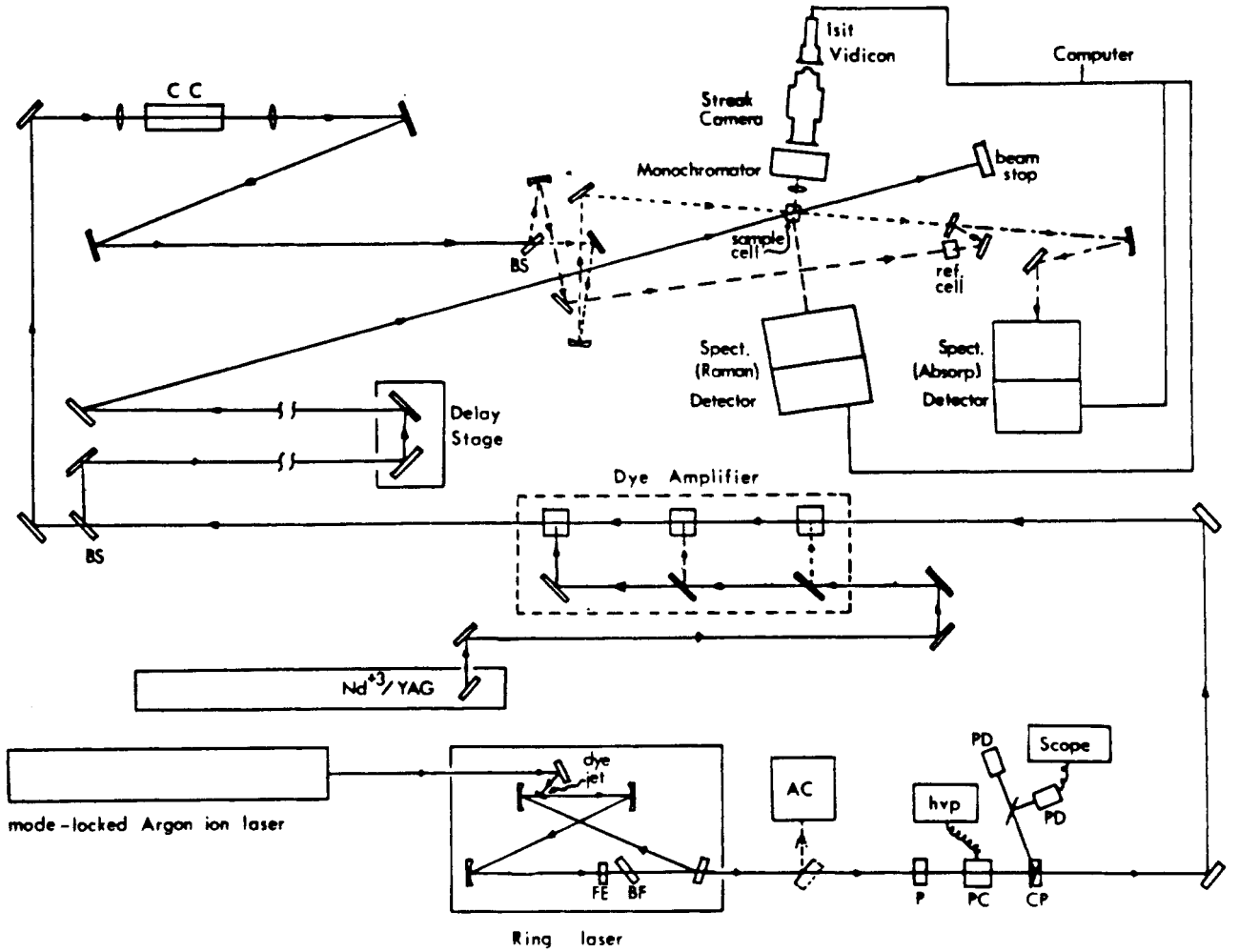


**Figure 1.** Schematic diagram of a synchronously pumped dye laser system: FE, fine etalon; BF, birefringent filter; AC, autocorrelator; P, polarizer; PC, Pockels cell; CP, crossed polarizer; hvp, high-voltage pulser; PD, photodiode; BS, beam splitter; CC, continuum cell.

amplified to powers of gigawatts, and easily operated at repetition rates of ~10 Hz. Each of these types of systems can be designed for emission, Raman, or absorption spectroscopy.

Picosecond dye lasers have not enjoyed such widespread use as solid-state lasers probably because of the relatively low-energy content of the pulses initially emitted ($\sim 10^{-9}$ J), the cost, and the elaborate schemes required to amplify them. In spite of this disadvantage, the possibility of generating tunable picosecond pulses and the variety of time-resolved processes that can subsequently be studied have stimulated a continuous increase in the utilization of these laser systems. In view of the many available descriptions in the literature of the solid-state systems, we shall restrict our description to the design of the synchronously pumped dye laser used in our laboratory, which to a large extent is utilized by many investigators. A number of the elements and techniques described in this Account for the picosecond dye laser system are analogous to those employed in the solid-state lasers that have been described previously.[2]

The tunable pulse generating source in this system (Figure 1) is a ring dye laser synchronously pumped by an actively mode-locked argon ion laser. The argon ion laser is mode locked by an acousto-optic modulator driven by an ultrastable frequency generator (~0.25 ppm) at 123 MHz, producing 150-ps pulses of 514.5-nm light with an average power of as much as ~4 W. These 150-ps pulses pump a ring dye laser and generate a series of picosecond pulses separated by 4 ns. The ring laser, a travelling-wave laser, has a conversion output of as much as 4 times that possible with a traditional standing wave dye laser. An average power of ~100 mW between ~570 and ~620 nm may be generated with rhodamine 6G (R6G). These short pulse widths are measured usually by means of an autocorrelator.[3] However, caution should be exercised because this method for measuring picosecond pulses may possess several shortcomings, which might lead to erroneous results.[4] Slight changes (on the order of micrometers) in the length of the cavity of the ring laser dramatically affect the pulse- width (~1–~20 ps) and may even generate multiple picosecond pulses separated by several picoseconds. Multiple-pulse generation may only very subtley manifest itself in the autocorrelation trace and may not be detected at all unless a streak camera is used to measure single pulses.[4]

The inherently low intensity of the ring dye laser pulses and their temporal separation of 4 ns requires that single pulses are selected and then amplified for most chemical research. The selection of a single pulse is achieved by means of a Pockels cell and crossed Glan

(2) Rentzepis, P. M. *Science* **1978**, *202*, 174.

(3) "Ultrashort Light Pulses"; Shapiro, S. L., Ed., Springer-Verlag: Heidelberg, 1977.

(4) Shapiro, S. L.; Cavanaugh, R. R.; Stephenson, J. C. *Opt. Lett.* **1981**, *6*, 470.

polarizers. The Pockels cell consists of a KDP crystal that becomes birefringent when a high-voltage pulse (~8 kV) is applied. The pulses emitted by the ring laser are horizontally polarized and pass through the first polarizer and the Pockels cell but are rejected by the second (crossed) polarizer. Application of the high voltage to the Pockels cells causes the polarization of a pulse to be rotated by 90° and thus transmitted by the crossed polarizer.

The selected pulse is amplified (~$10^6$ times) by means of a dye amplification system. The selection of the picosecond pulse and the triggering of a $Nd^{3+}$:YAG laser operating at 10 Hz (10-ns pulses of the second harmonic, 532 nm) are timed such that the picosecond pulse arrives at a series flowing dye cells (R6G) as the dye is pumped by the 532-nm pulse. The 532-nm pulse is split in a ratio to achieve optimum amplification. Unwanted emission is eliminated by focusing the amplified pulse after each dye amplifier cell through a saturable absorber.

The amplified pulse can be used directly for emission spectroscopy. For absorption spectroscopy the pulse is split into two, an excitation pulse and probe continuum generating pulse. Similarly for Raman spectroscopy, two pulses of different wavelengths are used for excitation and scattering pulses. The laser system presented in Figure 1 is of sufficient versatility to be configured for any of these forms of spectroscopy. Fluorescence spectra and decay can be detected by using a monochromator, streak camera, vidicon, optical multichannel analyzer (OMA) assembly. Time-resolved absorption and Raman spectra are detected with a spectrometer, reticon, and OMA assembly. The data is then sent to and processed by a minicomputer. The capability of obtaining a large number of data points and extensive data analysis and signal averaging allows this system to achieve rather high versatility and reliability of data. In addition, the dye laser system permits excitation with 1-ps FWHM pulses over the range of wavelengths from ~200 to ~800 nm by means of various dyes, second harmonic generation, and Raman shifting.

## Applications of Picosecond Spectroscopy

Chemical applications of time-resolved emission and absorption spectroscopy in the picosecond time regime have revealed subtleties and complexities that are present within chemical systems subjected to photoexcitation. Phenomena that were inferred from observations utilizing less time sensitive chemical probes are now observed directly with picosecond spectroscopy. Several illustrative examples of the present capabilities of picosecond spectroscopy are now discussed for chemical reactions that feature dynamic changes in fluorescence as a function of solvent polarity and viscosity, conformational changes during the course of a chemical reaction, predissociation mechanisms, and radical formation.

## Relaxation Dynamics of Excited States of *p*-(Dimethylamino)benzonitrile

The observation of dual fluorescences from (dimethylamino)benzonitrile (DAB) in polar solvents has stimulated many studies on the nature and kinetics of the emitting states. Many interpretations of this anomalous phenomenon have appeared.[5-9] Both

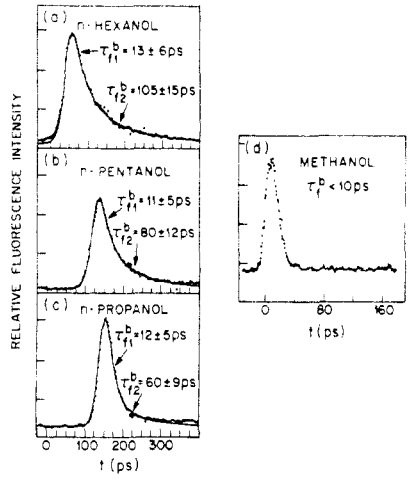


**Figure 2.** Time resolved b* fluorescence intensities of ~$10^4$ M solutions of DAB excited by 266-nm excitation pulses in 1-hexanol, 1-pentanol, 1-propanol, and methanol at 20 °C (from Huppert et al.[18]). Each trace was averaged over five to eight laser pulses.

fluorescence bands are polarized parallel to the plane of the benzene ring[10] with the maximum of the band designated a occurring at ~470 nm in polar solvents and the maximum of the b band occurring at ~350 nm in both polar and nonpolar solvents. A highly polar excited state is believed to be responsible for the a band. These bands have been shown not to correspond to low-lying $^1(\pi,\pi^*)$ states, nor to the first absorption band in DAB.[10,11] Recent steric evidence[11] supports the assignment of the emitting state, a*, to a strongly dipolar, twisted internal charge-transfer singlet state, $^1$(TICT),[12] which torsionally relaxes to a conformation in which the phenyl ring and the dimethylamino group are mutually perpendicular.

The results of oxygen fluorescence quenching studies suggest that a* and b* are formed consecutively and not competitively in acetonitrile solution.[13,14] The b* fluorescence lifetime of DAB in acetonitrile was estimated to be 10 ps[13] and appeared to be limited by the rate of internal rotation and not solvent viscosity since the time required for solvent reorientation is only ~1.5 ps.[15] Alternatively, when a different kinetic model is assumed in which a* and b* take part in a reversible equilibrium, results of quenching experiments imply a half-life as short as ~2 ps for DAB in methylene chloride.

Direct measurements of fluorescence decay rates by means of picosecond spectroscopy provide kinetic data

(5) Lippert, E.; Luder, W.; Moll, F.; Nagele, W.; Boos, H.; Prigge, H. Pr. H.; Seibold-Blankenstein, I. *Angew. Chem.* **1961**, *73*, 695.
(6) Lippert, E.; Luder, M.; Boos, H. In "Advances in Molecular Spectroscopy"; Mangini, A., Ed., Pergamon: New York, 1962; p 443.
(7) Siemarczuk, A.; Grabowski, Z. R.; Krowczynski, A.; Asher, M.; Ottolenghi, M. *Chem. Phys. Lett.* **1977**, *51*, 315.
(8) Kosower, E. M.; Dodiuk, H. *J. Am. Chem. Soc.* **1976**, *98*, 924.
(9) Grabowski, Z. R.; Rotkiewicz, K.; Siemiarczuk, A.; Cowley, D. J.; Baumann, W. *Nouv. J. Chim.* **1979**, *3*, 443.
(10) Rotkiewicz, K.; Grellmann, K. H.; Grabowski, Z. R. *Chem. Phys. Lett.* **1973**, *19*, 315.
(11) Rotkiewicz, K.; Grabowski, Z. R.; Krowczynski, A.; Kuhnle, W. *J. Lumin.* **1976**, *12/13*, 877.
(12) Grabowski, Z. R.; Rotkiewicz, K.; Siemiarczuk, A. *J. Lumin.* **1979**, *18/19*, 420.
(13) Rotkiewicz, K.; Grabowski, Z. R.; Jasny, J. *Chem. Phys. Lett.* **1975**, *34*, 55.
(14) Kirkor-Kaminska, E.; Rotkiewicz, K.; Grabowska, A. *Chem. Phys. Lett.* **1978**, *58*, 379.
(15) Whittenburg, S. L.; Wang, C. H. *J. Chem. Phys.* **1977**, *67*, 4255.

that do not rely on a previously assumed kinetic model as does the interpretation of the fluorescence quenching data. Struve et al.[16] observed a risetime of ~40 ps for the a* fluorescence of DAB at ~470 nm in methanol, ethanol, and 1-butanol and a longer risetime in the more viscous cyclohexanol. Other picosecond results substantiate these data.[17]

Using the fourth harmonic (266 nm, 20-ps FWHM) of a $Nd^{3+}$:YAG laser for sample excitation and a streak camera for detection of the ultrafast fluorescence events, Huppert et al.[18] measured a* fluorescence risetimes of DAB and the a* formation kinetics by monitoring b* fluorescence decay that previously[16,17] could not be detected as a result of picosecond spectrometer limitations. This study was performed over a wide range of solvents and temperatures. Figure 2 illustrates the b* fluorescence decays in several hydroxylic solvents of different viscosity. A monophotonic absorption was implied by the linear relationship between fluorescence intensity and laser pulse energy density. Under experimental conditions in which only b* fluorescence was observed, the b* state appeared promptly (risetime, $\tau_r^b$, < 10 ps) in such solvents as methanol, 1-hexanol, 1-dodecanol, methylcyclohexane, ethylene glycol, and glycerol. The decays of b* fluorescence were found to be biphasic in all linear alcohols (except methanol where $\tau_f^b$ was within the time resolution of the experiment) and to possess a long component fluorescence lifetime that was linearly related to the respective solvent viscosity. In addition to the case of methanol solvent, pulse-limited fluorescence decay also was observed for the polar aprotic solvents, dimethyl sulfoxide, *N,N*-dimethylformamide, and acetonitrile, whose room-temperature viscosities are less than 2.5 cP. The only solvents for which viscosity dependent fluorescence lifetimes ($\tau_f^b$) were not observed were such nonpolar aprotic solvents as methylcyclohexane and diethyl ether ($\tau_f^b$ = 1.8 and 3.2 ns, respectively at 25 °C) in which, as known previously,[5,6] no a* fluorescence was observed.

Using filters which pass wavelengths ≥ 520 nm, Huppert et al.[18] found that the a* fluorescence risetimes ($\tau_r^a$) are the same as the b* fluorescence lifetimes ($\tau_f^b$), within experimental error, for the solvents 1-dodecanol, 1-decanol, 1-hexanol, and 1-pentanol (Figure 3). This complementary relationship confirmed the previous conclusion made on the basis of fluorescence quenching data[13]—the b* state is therefore assigned to a kinetic precursor of the a* state in many polar solvents. The a* decay times ($\tau_f^a$ = 1.4, 3.7, 3.4, and 3.6 ns in methanol, acetonitrile, 1-hexanol, and 1-dodecanol, respectively) were measured to be single exponential and exhibited a marked temperature dependence. The temperature dependence was attributed to a previously unacknowledged thermally activated nonradiative process. Also, for the first time, this study revealed biexponential b* decays and a* risetimes. The long-time component was attributed to normal decay and risetime of the bands, while the short-time component was interpreted as reflecting the microscopic solvent reorientation required for solvation of these polar states.

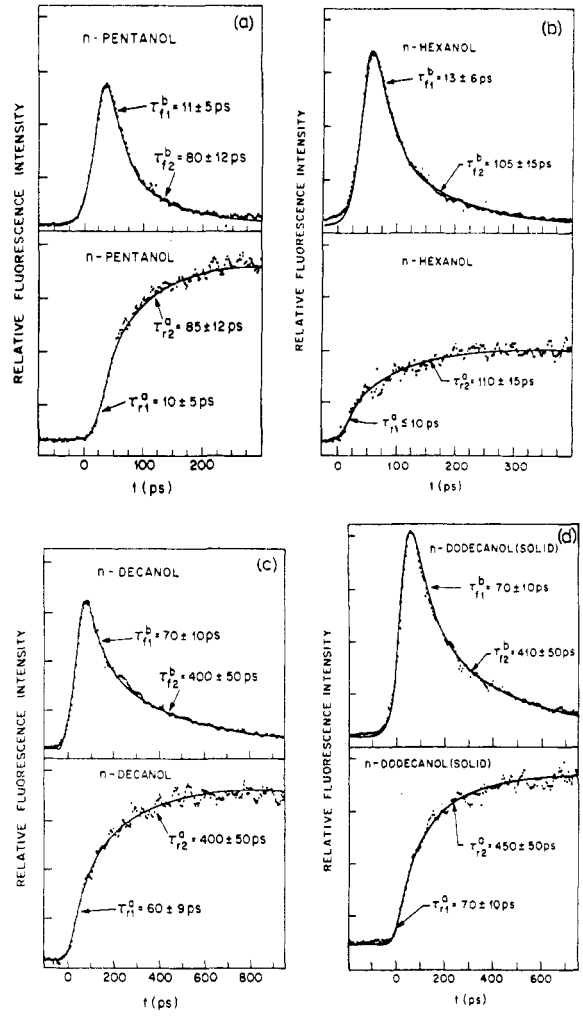


**Figure 3.** Comparisons of b* fluorescence decay times $\tau_f^b$ to a* fluorescence risetimes $\tau_f^a$ for DAB in (a) 1-pentanol, (b) 1-hexanol, (c) 1-decanol; (d) 1-dodecanol, all at 20 °C (from Huppert et al.[18]).

To understand further the conformational changes and their mechanism, a series of experiments were performed that contributed to further understanding of torsional motion of molecules in solution.

## Torsional Motion in Excited States

In addition to fluorescence and phosphorescence, radiationless processes manifested in the form of geometric changes of the molecular structure play an important role in photochemical processes. Such processes have of course been studied since the conception of picosecond spectroscopy.[19] However, of the various radiationless transitions, excited-state conformational relaxation is probably one of the least studied, even though such processes are very common and of significant importance in photochemical reactions in which starting material and product differ markedly in structure.[20,21] Early published results revealed some

(16) Struve, W. S.; Rentzepis, P. M. *J. Chem. Phys.* **1974**, *60*, 1533.
(17) (a) Struve, W. S.; Rentzepis, P. M; Jortner, J. *J. Chem. Phys.* **1973**, *59*, 5014. (b) Struve, W. S.; Rentzepis, P. M. *Chem. Phys. Lett.* **1974**, *29*, 23.
(18) Huppert, D.; Rand, S. D.; Rentzepis, P. M., Barbara, P. F.; Struve, W. S.; Grabowski, Z. R. *J. Chem. Phys.* **1981**, *75*, 5714.

(19) (a) Barbara, P. F.; Brus, L. E.; Rentzepis, P. M. *Chem. Phys. Lett.* **1980**, *69*, 447. (b) Barbara, P. F.; Rentzepis, P. M.; Brus, L. E. *J. Chem. Phys.* **1980**, *72*, 6802. (c) Noe, L. J.; Degenkolb, E. O.; Rentzepis, P. M. *Ibid.* **1978**, *68*, 4435. (d) Spears, K. G.; El-Manguch, M. *Chem. Phys.* **1977**, *24*, 65. (e) Lin, H. B.; Topp, M. *Chem. Phys. Lett.* **1979**, *64*, 452.
(20) For examples involving cis–trans isomerization, see the following: (a) Fischer, G.; Seger, G.; Muszkat, K. A.; Fischer, E. *J. Chem. Soc., Perkin Trans. 2* **1975**, 1569. (b) El-Bayoumi, M. A.; Abdel-Halim, F. M. *J. Chem. Phys.* **1968**, *48*, 2536. (c) Stegemeyer, H. *Chem. Ber.* **1968**, *72*, 335. (d) Kordas, J.; El-Bayoumi, A. *J. Am. Chem. Soc.* **1974**, *96*, 3043. (e) DeBoer, C. O.; Schlessinger, R. Y. *Ibid.* **1968**, *90*, 803. (f) Saltiel, J.; Zafiriou, O. C.; Megarity, E. D.; Lamola, A. A. *Ibid.* **1968**, *90*, 4759.

Table I
Kineti c Processes for TPE Relaxation[23]

| assignment | proposed pathway (see Scheme II) | manifestation | $T$, K | $\tau^{-1}$ |
|---|---|---|---|---|
| vibrational relaxation | $S_{1A}^* \rightarrow S_{1A}$ | spectral shift (time dependent) | 4 | $\sim 10^{11}$ |
| | | | >50 | $>10^{12}$ |
| torsional rearrangement | $S_{1A} \rightarrow S_{1B}$ | spectral shift (time dependent) | 4-90 | $<10^9$ |
| | | | 110-160 | $10^9$-$10^{10}$ |
| | | | 170-293 | $10^{10}$-$10^{12}$ |
| torsionally induced electronic radiationless decay (major component) | $S_{1B} \rightarrow S_{1C} \rightarrow S_{0C}$ | fluorescence decay kinetics (major component) | 4-130 | $<10^8$ |
| | | | 140-293 | $10^9$-$10^{10}$ |
| torsionally induced electronic radiationless decay (minor component) | $S_{1B} \rightarrow S_{1B}' \rightarrow S_{1C} \rightarrow S_{0C}$ or $\rightarrow S_{1C} \rightarrow S_{0C}$ $S_{1B} \rightarrow S_{1C}' \rightarrow S_{0C}'$ | fluorescence decay kinetics (minor component) | 4-130 | $<10^8$ |
| | | | 140-293 | $10^8$-$10^{10}$ |

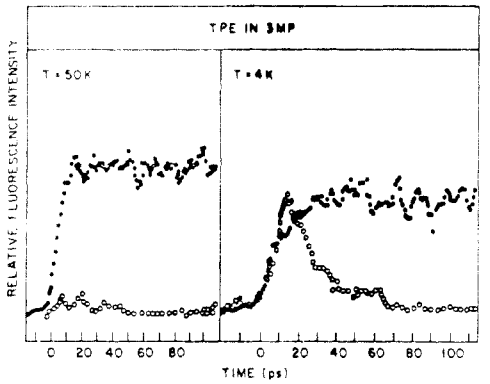


**Figure 4.** Low-temperature time-resolved fluorescence intensities of TPE in 3-methylpentane at 380 (open circles) and 420–600 nm (solid circles). Left figure, $T$ = 50 K; right figure, $T$ = 4 K (from Barbara et al.[23]).

of the general features of excited-state conformational changes.[22] More detailed information has recently been obtained by means of picosecond fluorescence spectroscopy. This technique has been utilized successfully to measure directly the growth and decay of emission associated with various conformational changes that a molecule undergoes upon photoexcitation.

An example of this type of study was performed by Barbara et al.[23] In these experiments, picosecond fluorescence spectroscopy was used to observe the photochemical dynamics of tetraphenylethylene (TPE) as a function of viscosity and temperature. TPE was excited at 355 nm in several solvents, including 3-methylpentane, Decalin, phenol, ethylene glycol, and triacetin at temperatures ranging from 4 to 293 K and viscosities from 0.31 (3-methylpentane) to ~28 cP (triacetin). The emission spectra of TPE and fluorescence decay kinetics as a function of temperature and solvent viscosity were recorded by means of a streak camera and OMA coupled to a minicomputer for data processing.

In these studies, at least four distinct chemical processes were identified for the excited-state relaxation

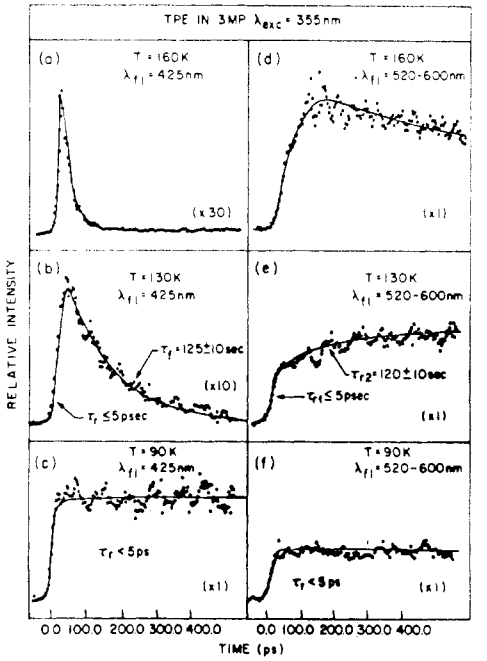


**Figure 5.** Formation and decay kinetics of TPE fluorescence as a function of temperature (solvent viscosity) and emission wavelength. Solid lines represent computer fits (from Barbara et al.[23]).

of TPE (Table I). The first process, vibrational relaxation, was directly observable by low-temperature, time-resolved fluorescence spectroscopy. Excitation with a 355-nm pulse revealed the presence of unrelaxed fluorescence at 380 nm, possessing a risetime of ≤4 ps and a decay time of 15 ± 5 ps (Figure 4). The kinetics were found to be identical over the range of wavelengths from 420 to 600 nm. At 4 K, the two risetimes depicted in Figure 4 with time constants of ~4 and ~15 ps were interpreted as originating from a hot vibrational energy distribution and the relaxed level, respectively. Such behavior at low temperature is quite similar to tetracene, previously reported by Barbara et al.[19b] At temperatures >50 K, a <4-ps risetime was observed for both components of TPE, in agreement with the characteristic behavior of other similar molecular species.[19a,b,22a,23] Figure 5 presents an example of the data obtained for time- and wavelength-resolved fluorescence that provided evidence for a second process, the existence of a torsional rearrangement in the excited state. If a torsional rearrangement were occurring in the excited state, we should expect to observe a fluorescence spectrum indicative of an unrearranged geometry, under appropriate viscosity conditions, in which the short-wavelength region (for TPE, ~425 nm)

(21) For examples involving intramolecular cyclization, see the following: (a) Billen, D.; Bocus, N.; De Schryver, F. C. *J. Chem. Res. Synop.* **1979**, 79. (b) Mallory, F. B.; Gordon, J. T.; Wood, C. S. *J. Am. Chem. Soc.* **1963**, *85*, 828; **1964**, *86*, 3094; (c) Fischer, E.; Muszkat, K. A. *J. Chem. Soc. B* **1967**, 662. (d) Fischer, E.; *Fortschr. Chem. Forsch.* **1967**, *7*, 605.

(22) (a) Barbara, P. F.; Brus, L. E.; Rentzepis, P. M. *J. Am. Chem. Soc.* **1980**, *102*, 5631. (b) Heisel, F.; Miehl, J. A.; Sipp, B. *Chem. Phys. Lett.* **1979**, *61*, 115. (c) Taylor, J. R.; Adams, M. C.; Sibbett, W. *Appl. Phys. Lett.* **1979**, *35*, 590. (d) Greene, B. I.; Hockstrasser, R. M.; Weisman, R. B. *Chem. Phys. Lett.* **1979**, *62*, 427. (e) Greene, B. I.; Hockstrasser, R. M.; Weisman, R. B. *J. Chem. Phys.* **1979**, *71*, 544. (f) Klingenberg, H. H.; Lippert, E.; Rapp, *W. Chem. Phys. Lett.* **1973**, *18*, 417. (g) Rapp, W. *Ibid.* **1974**, *27*, 187.

(23) Barbara, P. F.; Rand, S. D.; Rentzepis, *P. M. J. Am. Chem. Soc.* **1981**, *103*, 2156.

Scheme I[23]

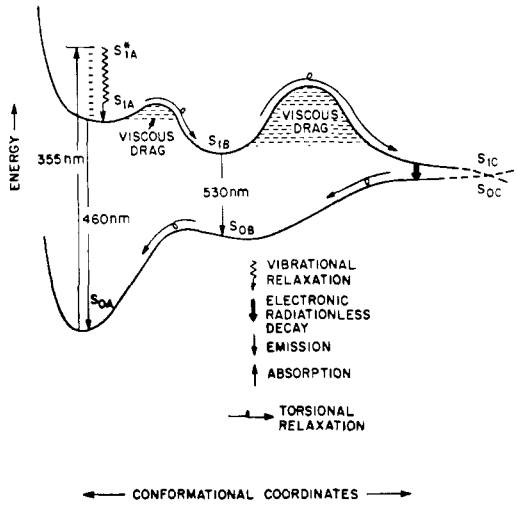


would appear instantaneously and decay at a rate that reflects time required for the rearrangement. Also, the long-wavelength region of the spectrum (for TPE, ~550 nm) corresponding to the rearranged geometry should appear with a risetime equal to the fluorescence lifetime of the short-wavelength region. The involvement of such a rearrangement is, in fact, clearly shown by the data depicted in Figure 5. A noteworthy point is that the data strongly suggest that the rearrangement responsible for the bathochromic shift is not the rearrangement responsible for inducing the radiationless decay. This is supported by the fact that the long-wavelength fluorescence decays much more slowly than the short-wavelength fluorescence is converted to the long-wavelength emission.

The additional kinetic processes observed by Barbara et al.[23] were assigned to torsionally induced electronic radiationless decays. Over the temperature range of 193–293 K, multiexponential fluorescence decays were observed that indicated that the radiationless decay of TPE involves, in addition to a dominant component, at least one other minor decay.

The proposed kinetic model that consolidates these results is outlined in Scheme I (see also Table I for proposed pathways). The fluorescence spectra and decay channels and lifetimes of TPE indicate a relaxation mechanism whose complexity is possibly the norm for most large molecules and photochemical reactions.

## Predissociation of Haloaromatics

Detailed studies of intersystem crossing and predissociation of several haloaromatics have been performed lately by Struve and co-workers[24a] and Huppert et al.[24b] Transient emission and absorption kinetic and spectral data obtained in the picosecond time regime have been reported that clarified the channels of energy dissipation and predissociation available to these molecules. Prior to these investigations, several uncertainties existed concerning the mechanism and states involved in photodissociation of haloaromatics. Previous work on haloaromatics demonstrated that intersystem crossing occurs from an excited singlet state to a lower lying triplet state. Ermolaev and Svitashev[25] studied the room-temperature fluorescence and low-temperature phosphorescence in solid glasses of 1-chloro-, 1-bromo-, and 1-iodonaphthalene. From the quantum-yield measurements and the natural radiative lifetimes of the states involved, the fluorescence lifetimes of the excited singlet states of the haloaryl compounds could be calculated.

Pavlopoulos et al.[26] reported that a least two phosphorescence "subspectra" could be observed in such species that differ in polarization and exhibit enhanced phosphorescence by heavy-atom substitution. By recording $T_n \leftarrow T_1$ absorption spectra, it became possible to measure the decay rates of the triplet states of naphthalene, anthracene, and phenanthrene and their halogenated derivatives at room temperature in cyclohexane and viscous paraffin solutions. While $T_n \leftarrow T_1$ spectra were observed for bromo- and chloronaphthalene ($\lambda_{max}$ 425 nm), no triplet absorption spectrum was observed for iodonaphthalene dissolved in either cyclohexane or glycerol. The inability to observe triplet spectra of iodonaphthalene was attributed to the possibility of a triplet lifetime of less than 10 $\mu$s. Estimates made by Sandros et al.[27] place the triplet lifetimes of 1-iodo- and 2-iodonaphthalene at 10 and 1100 ns, respectively. Investigations of aromatic halides by Wilkinson[28] and Levy et al.[29] demonstrated that dissipation of energy from the triplet state proceeds via cleavage of the carbon–halogen bond. However, their studies also indicated that dissociation could occur directly from the excited singlet state. Pulse radiolysis studies, performed by Grieser and Thomas,[30] revealed a rather unusual temperature dependence of the triplet-state lifetime that was attributed to the crossing of the potential energy barrier from the triplet state to a dissociative $^3(\sigma,\sigma^*)$ state. Using picosecond emission spectroscopy, Laigusa et al.[31] measured the intersystem-crossing rate between the lowest singlet and triplet states of 1-chloronaphthalene ($(5.9 \pm 0.8) \times 10^8$ s$^{-1}$) and 1-bromonaphthalene ($(1.5 \pm 0.3) \times 10^{10}$ s$^{-1}$). Again the very short lifetime of the singlet state of 1-iodonaphthalene presented difficulties. Since the fluorescence intensity of 1-iodonaphthalene was too weak to be measured, the intersystem-crossing rate, in turn, could not be measured.

Estimates of the photodissociation rates of haloaromatics have been made by Freedman et al.[32] by way of molecular beam studies. The lifetimes of iodobenzene, 1-iodonaphthalene, and 2-iodonaphthalene were determined to be approximately 0.5 ps. The lifetime of methyl iodide was found to be only 0.07 ps. The corresponding aryl bromides were estimated to possess lifetimes that are approximately 2 orders of magnitude longer than aryl iodides. They[32] concluded that photodissociation proceeds via intersystem crossing

(24) (a) Pineault, R. L.; Morgante, C. G.; Struve, W. S. *J. Photochem.* **1981**, *17*, 435. (b) Huppert, D.; Rand, S. D.; Reynolds, A. H.; Rentzepis, P. M. *J. Chem. Phys.* **1982**, *77*, 1214. (c) Kelley, D. F.; Milton, S. V.; Huppert, D.; Rentzepis, P. M. *J. Phys. Chem.* in press.

(25) Ermolaev, V. L.; Svitashev, K. K. *Opt. Spectrosc.* **1959**, *7*, 399.

(26) Pavlopoulos, T.; El-Sayed, M. A. *J. Chem. Phys.* **1964**, *41*, 1083.

(27) (a) Sandros, K. *Acta Chem. Scand.* **1964**, *18*, 2355. (b) Sandros, K.; Backstrom, H. *Acta Chem. Scand.* **1962**, *16*, 958.

(28) Wilkinson, F. *J. Phys. Chem.* **1962**, *66*, 2564.

(29) Levy, A.; Meyerstein, D.; Ottolenghi, M. *J. Phys. Chem.* **1973**, *77*, 3044.

(30) Grieser, F.; Thomas, T. K. *J. Chem. Phys.* **1980**, *73*, 2115.

(31) Saigusa, S.; Azumi, T.; Sumitari, M.; Yoshihara, K. *J. Chem. Phys.* **1980**, *72*, 1713.

(32) Freedman, A.; Yang, S. C.; Kawasaki, M.; Bersohn, R. *J. Chem. Phys.* **1980**, *72*, 1028.

Table II
Room-Temperature (~20 °C) Fluorescence Lifetimes of Halonaphthalenes and Haloanthracenes in Hexane[24b]

| sample | λ, nm | $\tau_f$, ps |
|---|---|---|
| 4,4-dibromobiphenyl | 265 | 30 |
| 4-bromobiphenyl | 265 | 35 |
| 1-bromonaphthalene | 265 | 75 |
| 1-bromo-4-methylnaphthalene | 265 | 80 |
| 1-bromo-2-methylnaphthalene | 265 | 72 |
| 2-bromonaphthalene | 265 | 150 |
| 1-(chloromethyl)naphthalene | 265 | 490 |
| 2-(bromomethyl)naphthalene | 265 | ND[a] |
| 1-chloronaphthalene | 265 | 2400 |
| 2-chloronaphthalene (zone refined >99%) | 265 | 3300 |
| 2-chloronaphthalene | 265 | 3500 |
| 9-bromoanthracene | 355 | 100 |
| 9,10-dibromoanthracene | 355 | 1300 |
| 2-iodoanthracene | 265 | 14 |
| 9-iodoanthracene | 265 | 35 |
| 2-iodoanthracene | 355 | 17 |
| 9-iodoanthracene | 355 | 55 |

[a] Not detected.

to the triplet state and then localization within the C–X bond and dissociation via

$$S_0 \rightarrow S_2(\pi,\pi^*) \rightarrow S_1(\pi,\pi^*) \rightarrow T(\sigma,\sigma^*) \rightarrow \text{dissociated species}$$

Since dissociation of iodoaryls was found to occur extremely rapidly, a few picoseconds, it was questioned whether relaxation to $S_1$ actually occurs or dissociation from the triplet states proceeds directly vis $S_2$.

At this time, the picosecond spectroscopic study of Huppert et al.[24b] was performed in an effort to elucidate the mechanism of haloaromatic photodissociation. The combination of temporal information from $S_n \leftarrow S_1$, $T_n \leftarrow T_1$ time-resolved picosecond absorption and emission spectroscopy provided the means for detailed understanding of intersystem crossing and dissociation of haloaromatic compounds. The fluorescence lifetimes of the aryl halides of the Huppert et al.[24b] study is reproduced in Table II.

A really detailed picture of a dissociation process can be drawn from the combination of the emission and absorption data. Prompt risetimes of the fluorescences provided evidence that relaxation within the excited-singlet manifold is completed within a few picoseconds, while the decay of fluorescence determines the relaxation rate of the singlet state. However, by themselves these data do not provide information concerning the state into which the energy is dissipated. This information was provided by the transient $S_n \leftarrow S_1$ and $T_n \leftarrow T_1$ absorption spectra (Figure 6). Finally, unequivocal evidence for the pathway leading to the dissociation process is provided by the lifetime of fluorescence decay coupled with the rates of disappearance of the $S_n \leftarrow S_1$ transient absorption and of appearance of the $T_n \leftarrow T_1$ spectrum.

The transient absorption data obtained within the first 500 ps after excitation coupled to the emission lifetimes demonstrates that the pathway for photodissociation of haloaromatics (excited to upper vibronic levels of $S_1$) involves predominantly very prompt relaxation to $S_1$ followed by intersystem crossing to $T_1$ and subsequently dissociation. As expected, these measured intersystem-crossing rates decrease from iodo to bromo to chloro substitution. The triplet-state population did not disappear within the first 500 ps after excitation for bromo and chloro substituents, indicating that dissociation from the triplet state is longer than 500 ps. Photodissociation of iodoanthracene, the aryl iodide studied in their work, is extremely fast and believed to proceed via the triplet state. The rate of dissociation being orders of magnitude faster than the aryl bromide or chloride is in agreement with the Bersohn proposal.[32] While picosecond studies have provided detailed information about the mechanism of haloaromatic photodissociation, some questions still remain with regard to the fragment formation mechanism and are addressed in a recent paper by Kelley et al.[24c]

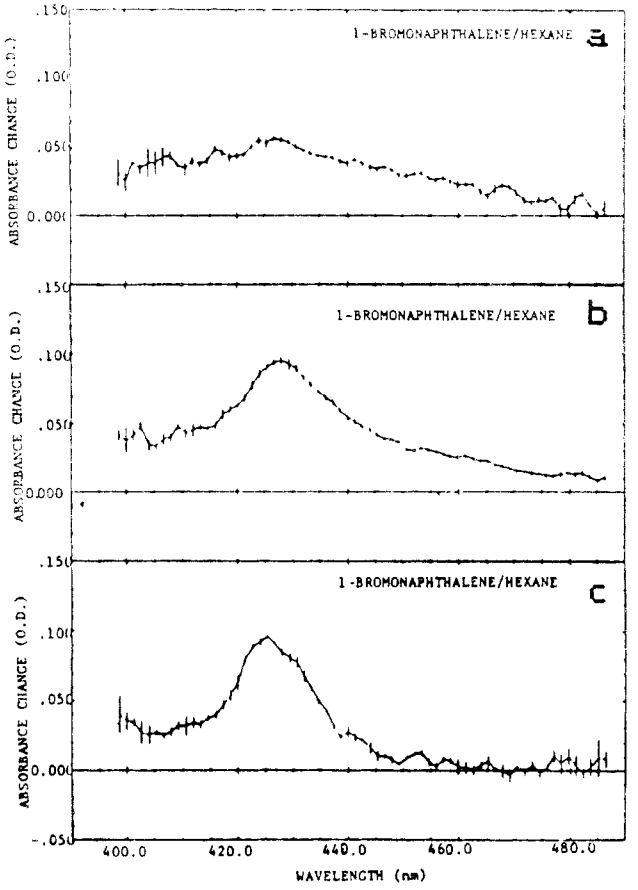


**Figure 6.** Representative transient absorption spectra. Transient absorption spectra of 1-bromonaphthalene in hexane at room temperature (from Huppert et al.[24b]).

## Transient States of TMM Derivatives

Another chemical species that has recently come under investigation with picosecond fluorescence spectroscopy is the trimethylenemethane (TMM) derivative, 2-isopropylidenecyclopentane-1,3-diyl.[33] The trimethylenemethane biradical has been the subject of extensive theoretical and experimental studies.[34] While observations of triplet ground-state TMM itself[35] and several derivatives,[36] by EPR spectroscopy, have been

(33) (a) Kelley, D. F.; Mazur, M. R.; Rentzepis, P. M.; Berson, J. A. *J. Am. Chem. Soc.* **1982**, *104*, 3764. (b) Kelley, D. F.; Rentzepis, P. M. *Ibid.* **1983**, *105*, 1820.

(34) For recent reviews, see the following: (a) Berson, J. A. *Acc. Chem. Res.* **1978**, *11*, 446. (b) Berson, J. A. In "Diradicals"; Borden, W. T., Ed.; Wiley: New York, 1982.

(35) Dowd, P. *Acc. Chem. Res.* **1972**, *5*, 242 and references cited therein.

(36) Platz, M. S.; McBride, J. M.; Little, R. D.; Harrison, J. J.; Shaw, A.; Potter, S. E.; Berson, J. A. *J. Am. Chem. Soc.* **1976**, *98*, 5725.

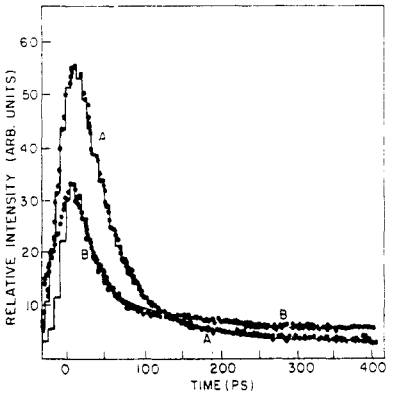


**Figure 7.** Fluorescence intensity (>310 nm) vs. time for diazene 1 (A) and diazene 2 (B) in hexane at room temperature. Solid lines are calculated biphasic curves with decay times of 38 and 280 ps for 1 and of 25 and 310 ps for 2. No relationship between the two curves is implied since the intensities are not normalized (from Kelley et al.[33b]).

reported in the literature, recently the singlet state of a derivative of this biradical has been established as an intermediate on its potential energy surface. Evidence for the existence of singlet 2-isopropylidenecyclopentane-1,3-diyl (**3S**) was based upon the kinetic analysis of Mazur and Berson[37] rather than direct observation.

It was only very recently, by means of picosecond fluorescence spectroscopy, that Kelley et al.[33] were able to observe the decay kinetics and emission spectra of transients generated by picosecond excitation of diazenes **1** and **2** in hexane solution at room temperature and in argon and xenon matrices at 4.2 K. In hexane

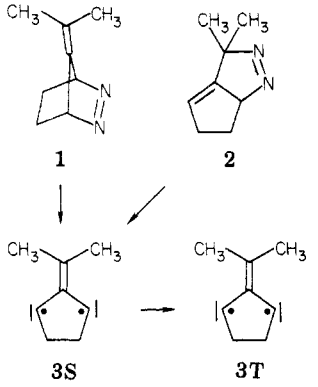


solution at room temperature, the fluorescence decay kinetics of both diazenes, excited by a picosecond pulse, were found to be biphasic, composed of a short-lived component with 38-ps lifetime for 1 and a 25-ps lifetime for 2 and long-lived component with a lifetime of 280 ps for 1 and 310 ps for 2 (Figure 7).

Kelley et al. assigned the short-lifetime events to predissociation of the excited singlet states of diazenes 1 and 2. It was proposed by these authors that the biradical is elevated to an excited singlet state by a second photon, **3S**,[35] either azo $\xrightarrow{2h\nu}$ **3S*** or azo $\xrightarrow{h\nu}$ **3S** $\xrightarrow{h\nu}$ **3S***. Either mechanism of formation results in a **3S*** state for both diazenes, which was found to decay subsequently with a lifetime of ~300 ps. Laser-induced fluorescence spectra obtained by photolysis of either diazene by a 25-ps pulse of 266-nm light indicated that

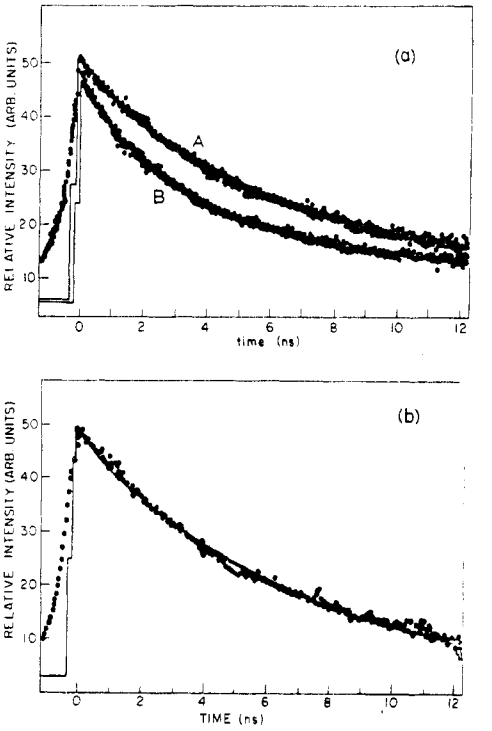


**Figure 8.** Time-resolved fluorescence intensities in argon (a) and xenon (b) matrices. In (a) diazene 1 corresponds to curve A and diazene 2 to curve B. Solid lines in (a) are calculated biphasic curves with decay times of 5.0 and 30 ns for A and of 3.1 and 30 ns for B. In (b) the decays of 1 and 2 are superimposed. The solid line in (b) is a computer fit based on a single-exponential decay of 6.5 ns (from Kelley et al.[33b]).

emission from **3S*** dominated the total spectra at room temperature in hexane. The laser-induced picosecond fluorescence decays and total emission spectra of matrix-isolated diazenes 1 and 2 were found to be dominated by the emission originating from the azo chromophore of the diazenes, which was concluded to be caused by the partial supression of deazetation at these very low temperatures, 4 K, in the inert-gas matrices.

In argon matrices, the fluorescence exhibited biphasic decays (Figure 8), with short component time constants of 5.0 and 3.1 ns for 1 and 2, respectively, and were assigned to the predissociative lifetime of these diazenes. Although the predissociative lifetimes of both diazenes are increased considerably from their own room-temperature values, their relative values show the same trend, namely, the predissociative lifetime of 1 remained longer than the corresponding value of 2. For the long-lived components, fluorescence lifetimes of 30 ns originate from the **3S*** state of both 1 and 2. The exact values of these lifetimes was not ascertained[33b] because of the inability of the streak camera to measure accurately longer lifetimes. However, the long decay lifetimes listed are on the order of that expected for the natural radiative lifetime **3S***.[38]

In xenon matrices, single-exponential fluorescence decays were observed for 1 and 2 with identical lifetimes of 6.5 ns (Figure 8). The total emission spectra of the species obtained from 1 or 2 in Xe matrices were very similar. This observation was interpreted to indicate a 2 → 1 isomerization occurring on a time scale that is fast compared to fluorescence decay.[33b] Since little, if

(37) Mazur, M. R.; Berson, J. A. *J. Am. Chem. Soc.* **1981**, *103*, 684.

(38) (a) Davis, J. H.; Goddard, W. A. *J. Am. Chem. Soc.* **1977**, *99*, 4242. (b) Strickler, S. J.; Berg, R. A. *J. Chem. Phys.* **1962**, *37*, 814.

any, emission associated with **3S*** was observed in Xe matrices, the lifetime of **3S*** was inferred to be <10 ns under these conditions. This supported the hypothesis proposed that intersystem crossing to a triplet state[34] is the main decay mechanism of **3S*** since such a process is expected to be facilitated by the external heavy-atom effect induced by a xenon matrix.

Kelley et al.[33b] have demonstrated that photolysis of diazenes **1** or **2** leads to the excited singlet state of the TMM derivative, **3S***. This is the first spectroscopic observation of a singlet biradical. In addition, their low-temperature, 4 K, matrix-isolation studies provided direct evidence of the predissociation mechanism and formation of the radical, and by means of consecutive excitation it was possible to identify the emission spectra of the species and measure its lifetime. Further studies with similar molecular species have enabled Kelley et al. to postulate with considerable certainty, based on experimental data, the mechanism of N=N scission and the differentiation between simultaneous and sequential C–N bond cleavage, a question that has been a long-term concern and study in reaction chemistry.

## Conclusion and Summary

The experimental investigations described here demonstrate the higher level of specificity and completeness, which picosecond emission and absorption spectroscopy permits in the understanding of mechanistic photochemistry. The constantly improving technology will allow a period of photochemical mechanistic revelation comparable to that of another era of great chemical progress, the golden age of physical organic chemistry that shed much light on the mechanistic aspects and general understanding of organic chemistry.

The versatility of the synchronously pumped dye laser system described above with the addition of picosecond Raman spectroscopy, with all of its structural information, enhances the repertoire of picosecond studies. The ultimate in the study of chemical reactions, the direct observation of bond cleavage and bond formation, is indeed a reality!